# Photophysics of Substituted 1,8-Naphthalimides Bound to a Poly(allylamine) Polymer

**Ti Cao† and S. E. Webber***

*Department of Chemistry and Center for Polymer Research, University of Texas at Austin, Austin, Texas 78712*

*Received April 19, 1990; Revised Manuscript Received June 6, 1990*

ABSTRACT: Poly(allylamine) has been modified by imidization of 0.02–0.08 mole fraction of available amino groups with 1,8-naphthalic anhydride or the corresponding 4-bromo and 4-sulfo derivatives. These latter chromophores have a strong absorption in the visible region (ca. 450 nm) and a high fluorescence quantum yield. The photophysical properties of the polymer-bound chromophores have been compared with model compounds. For the 4-substituted chromophores the fluorescence spectra of the polymer-bound species are similar to the model compounds but the fluorescence yield is decreased, and the multiexponential fluorescence decay implies a heterogeneous environment. The unsubstituted 1,8-naphthalimide exhibits excimer fluorescence when polymer-bound, even at 0.01 mole fraction loading. These results imply a strong tendency for the chromophores to aggregate, presumably intracoil. These photophysical properties are a function of pH and/or ionic strength, which affects the coil expansion. Fluorescence quenching was also studied as a function of pH and/or ionic strength, in an effort to elucidate the accessibility of the polymer-bound chromophores.

## Introduction

For a number of years the photophysics of chromophores bound to polymers has been an active research field, either from the point of view of elucidating polymer conformations and dynamics or from the point of view of providing a new class of photoreagents, including applications to "photon harvesting".[1] The range of chromophores used in these studies has not been particularly broad, with most work emphasizing aromatics such as naphthalene, phenanthrene, and anthracene. In the present article we report a study of a new class of polymer-bound chromophores based on the 1,8-naphthalimide moiety. One of the motivations for this work is to provide a polymer-bound chromophore that absorbs strongly in the visible region and that has a good fluorescent yield. This criterion is met by 4-substituted 1,8-naphthalimide model compounds, but upon attachment to a poly(allylamine)backbone the fluorescence yield is strongly diminished.

Substituted naphthalimide chromophores have been used as fluorescent probes for biological cells[2] and for laser dyes[3] and have been described in detail by Middleton et al.[4,5] Recently, Pardo et al.[6-11] carried out photophysical studies of some N-substituted 1,8-naphthalimides in which they reported solvent effects on the absorption and fluorescence spectra, fluorescence quantum yield, and lifetime[10] and, in the case of the 4-amino species, a strong shift in fluorescence upon protonation.[7,8] We have not found any literature on the photophysics of 4-bromo- and 4-sulfo-substituted 1,8-naphthalimides that constitute the fundamental chromophores of the present report.

Ionomers have interesting physical properties and have attracted considerable attention in polymer physics.[12] There have been several reports of fluorescence probes attached to water-soluble anionic polyacids to examine the morphological change of coils as a function of pH in aqueous solution.[13-15] In this paper, we describe the attachment of unsubstituted and 4-bromo- and 4-sulfo-1,8-naphthalimides to poly(allylamine) and their use as a fluorescence probe to monitor the response of a cationic polymer coil to the solution pH and ionic strength. We also present some fluorescence quenching results, which provide some insight as to the accessibility of the polymer-bound chromophores as a function of these same solution parameters.

† Permanent address: Institute of Chemistry, Academia Sinica, PRC.

## Experimental

**1. Synthesis of Model Compounds (BNPI, SNPI, NPI, 1; Chart I).** A total of 0.2 g of 4-bromo-1,8-naphthalic anhydride (BNA; Aldrich) was recrystallized from ethanol and dissolved in 7 mL of DMF with 1.0 g of propylamine (Aldrich). The condensation reaction was carried out at 60 °C under continuous stirring until the absorption peak at 352 nm, attributed to the anhydride, disappeared. The solvent and unreacted propylamine were removed by evaporation in vacuo. The product (BNPI) was separated from byproducts as the second main fraction with a 40-cm silica column (grade 62, 60–200 mesh) and 1:2 v/v THF/cyclohexane as the mobile phase.

A total of 0.2 g of 4-sulfo-1,8-naphthalic anhydride potassium salt (SNA; Aldrich) was dissolved in 7 mL of water and 1.0 g of propylamine added. The condensation was carried out for 48 h at 60 °C under continuous stirring. The yellow precipitate (SNPI) was separated from the solution by filtration, washed with water extensively, and dried in vacuo. Its purity was checked by TCL and absorption and emission spectra.

A total of 1.3 g of 1,8-naphthalic anhydride (Aldrich) and 0.4 g of propylamine were dissolved in 30 mL of absolute ethanol and refluxed with continuous stirring for 2 h. A dark material was removed by adding activated charcoal to the hot solution and filtering while hot. Upon cooling, a white crystalline material formed and was purified by recrystallization from absolute ethanol. This material was examined with IR spectroscopy, and it was determined that the anhydride carbonyl stretch at 1740 and 1770 $cm^{-1}$ had been replaced by the imide carbonyl stretch at 1660 and 1690 $cm^{-1}$.

In order to predict the type of redox quenching that these species might undergo, the redox potentials of the model compounds were determined by cyclic voltammetry by using an EG&G PARC Model 363 potentiostat and Model 175 universal programmer. All were found to undergo quasi-reversible oxidation and reduction. These data and the condition of measurement are presented in Table I.

**2. Synthesis of PBNAI-AA, PSNAI-AA, and PNAI-AA (2; Chart I).** A total of 1 g of poly(allylamine hydrochloride) (PAA) (Polysciences, Inc.) was dissolved in 20 mL of water followed by the addition of 0.5 g of $NaHCO_3$. A total of 0.2 g of BNA or SNA was dissolved in 5 mL of DMF, and these two solutions were mixed and refluxed under nitrogen for ca. 20 h until all anhydride was converted into imide, based on the changes

0024-9297/91/2224-0079$02.50/0 

**Chart I**

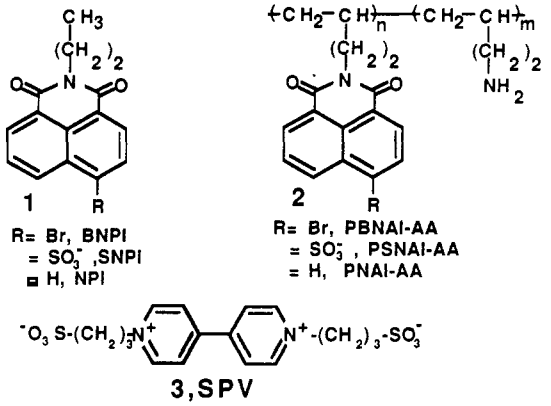




3,SPV

**Table I**
**Redox Potentials of Model Compounds**

| compd | redn,[a] V | oxidn,[a] V | solvent | electrolyte | ref electrode[a] |
|---|---|---|---|---|---|
| NPI | -1.4 | *b* | THF | 0.1 M TBAP[c] | SCE |
| BNPI | -1.61 | 1.11 | $CH_3CN$ | 0.1 M TBAP | SCE |
| SNPI | -1.56 | 1.16 | $CH_3CN$ | 0.1 M TBAP | SCE |
| SNPI | -1.66 | | THF | 0.1 M TBAP | SCE |
| SNPI | | 0.85 | $CH_3CN$ | 0.1 M TBAP | $Ag/Ag^+$(0.1 M) |
| naph | -2.51 | | THF | 0.1 M TBAP | SCE |
| naph | | 1.34[d] | $CH_3CN$ | 0.5 N $NaClO_4$<br>0.1 N $AgClO_4$ | $Ag/Ag^+$(0.1 M) |

[a] Working electrode is Pt foil. All redox processes were quasi-reversible. [b] No oxidation wave observed over the working range of the solvent. [c] Tetrabutylammonium perchlorate. [d] Value for naphthalene: Loveland, J. W.; Dimeler, G. R. *Anal. Chem.* **1961**, *33*, 1196.

in the absorption spectrum. The polymer solution was dialyzed with 6000–8000 molecular weight cutoff tubing (Spectrapor, Spectrum Medical Industries, Inc.) against water at 40 °C and pH 8.5 for 4 days to remove oligomer. The polymer sample was obtained after freeze-dry evaporation of the water. In the case of PSNAI-AA, the pH of the solution was adjusted to 3.5 by adding 3% HCl aqueous solution and the solution was dialyzed against water at 40 °C and pH 3.5 for 4 days. For both polymers ca. 3 mol % of chromophore was achieved. The preparation of PNAI-AA polymer was carried out in a similar fashion as the PBNAI-AA polymer. It was found that a higher loading of the unsubstituted 1,8-naphthalic chromophore on the polymer could be achieved than for the other substituted anhydrides. Two polymers were prepared with loadings of ca. 1 and 8 mol % (vide infra). Additionally some polymers were prepared with very low loading of the BNAI or SNAI chromophore (less than 1 chromophore per chain) for photophysical characterization.

It is worth noting that we initially attempted to carry out similar attachments of 3,4,9,10-perylenetetracarboxylic dianhydride (PTCD) and related derivatives, stimulated by the reports of the interesting photophysical properties of these compounds by Ford and Kamat.[16] However, we found it very difficult to carry out the same chemical attachment to poly(allylamine) as described above, primarily because of the low solubility of PTCD in water. Similarly, polymers containing aminostyrene did not result in a successful attachment, presumably because of the low chemical reactivity of the aromatic amine.

**3. Spectroscopic Instrumentation.** UV absorption spectra of solution were taken on a HP 8451 diode array spectrophotometer with 2-nm resolution, with the solvent being used as a reference.

The emission and excitation spectra were obtained on a SPEX fluorescence spectrophotometer with a 450-W xenon lamp, double monochromators for excitation and emission, a SPEX DM1B controller, and a cooled Hamamatsu R508 photomultiplier at right-angle geometry. The wavelength-dependent response of this system was determined by the measurement of a standard incandescent lamp obtained from the National Bureau of Standards. A slit width of 1.25 nm (band pass ca. 2.5 nm) was used for both excitation and emission monochromators. This system was used primarily for excitation spectra and quantum yield data. The fluorescence quantum yield was estimated by using the method of optically dilute solutions[17] in which the corrected spectrum of the unknown compound is compared to a standard, in this case $2.3 \times 10^{-4}$ M quinine bisulfate (Aldrich), which had been doubly recrystallized from dilute $H_2SO_4$. The quantum yield of this standard was assumed to be 0.544.[18]

The solvent dependence of the emission spectra was usually measured on a fluorescence spectrophotometer with a 150-W xenon lamp, a SPEX 1680 0.22-m excitation monochromator, a SPEX 1681 0.22-m spectrometer on the emission side, and a diode array detector (Tracor Northern 6100 series). A quartz fluorescence cell using a front-face excitation/observation geometry was used in all cases. The slit width was selected to be 1.25 and 0.25 mm (band pass ca. 2.25 and 7.2 nm) for the excitation and emission monochromators, respectively. The wavelength calibration of the emission spectrograph was carried out with an Oriel 6055 low-pressure mercury lamp. The diode array exposure time was 0.5 s, and background subtraction was carried out for all recorded emission spectra. The emission spectra presented are the average of 10 scans in all cases. For the studies of relative intensity changes, the intensity was integrated over ±25 nm around the peak wavelength as a measure of the emission intensity for a given spectral region.

Emission decays were measured on either a Photochemical Research Associates or a mode-locked laser, time-correlated single-photon-counting apparatus. For the former a Model 510 B flash lamp filled with hydrogen at ca. 380 Torr was employed to generate excitation pulses (<2 ns, fwhm) at a frequency of ca. 40 kHz. Excitation and emission wavelengths are selected with a Model H-10 Instruments S.A. monochromator. A thermoelectrically cooled Hamamatsu R928 photomultiplier was used to generate the stop pulses. An Ortec Model 918A multichannel buffer interfaced to an IBM AT was used to analyze the TAC output. The picosecond system consists of a mode-locked frequency-doubled Nd:YAG (Quantronix Model 416) synchronously pumping a cavity-dumped dye laser (Coherent Model 701-3D) circulating Rhodamine 6G. The Nd:YAG produces a series of pulses at 38 MHz and 532 nm with a pulse width <70 ps (fwhm). The dye laser output is tuneable in the range 570–620 nm and consists of pulses that are typically cavity-dumped at ca. 1.9 MHz with a fwhm of ca. 8 ps. For the present experiment the 586-nm output is frequency doubled with an angle-tuned KDP crystal. The fluorescence is collected at right angles, focused into a Model DH-10 Instruments S.A. double monochromator, and detected by a microchannel plate detector (Hamamatsu Model R-1564U-07) coupled to a Hewlett Packard Model 8447F amplifier. The single-photon-counting electronics for the picosecond system consist of a Tennelec TC 454 Quad CFD, Ortec Model 566 TAC, and an Ortec Model 918 MCB interfaced to an IBM AT. The instrument response function is ca. 70 ps (fwhm). With the present convolution techniques we believe we can extract a short lifetime component of ca. 250 ps to a precision of ±25 ps, based on the stability of the fit to different starting parameters and data weighting schemes. The decay profile was fit to a multiexponential decay function using standard reconvolution least-squares techniques.[19] The goodness of fit was evaluated by $\chi^2$ and the randomness of the distribution of residuals.

**4. Polymer Characterization by GPC.** GPC traces were taken on a Waters 510 HPLC with one Ultrahydrogel Linear column (Waters). A Perkin-Elmer LS-1 fluorescence detector and a Waters Associates differential refractometer R401 were connected in series as a dual detector. The signals from both detectors were simultaneously picked up and recorded by a computer. A wide band-pass filter (350–530 nm) was used for excitation, and the emission wavelength was selected to be 550 nm in the fluorescence detector. A pH 3.5 acetic acid/sodium acetate buffer solution was used as the eluant (0.1 M in both acetic acid and sodium acetate with $NaNO_3$ at 0.42 M to provide ionic strength). The elution rate was 0.5 mL/min with a sample size of 10 μL of 0.1 mg/mL of polymer solution. The GPC traces are shown in Figure 1. For both polymers the peak position and the onset of the fluorescence trace is similar to the refractive index trace, which indicates that all fluorescent chromophores are co-

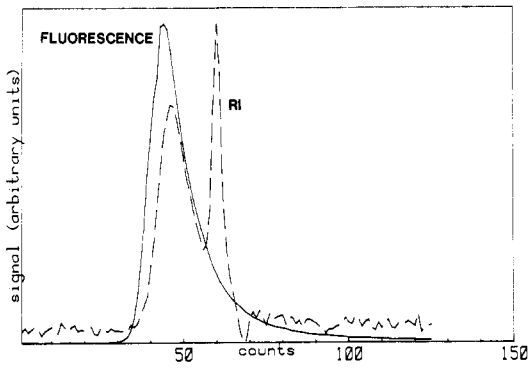


**Figure 1.** GPC trace for PSNAI-AA copolymer detected by differential refractometer (- -) and fluorescence (—).

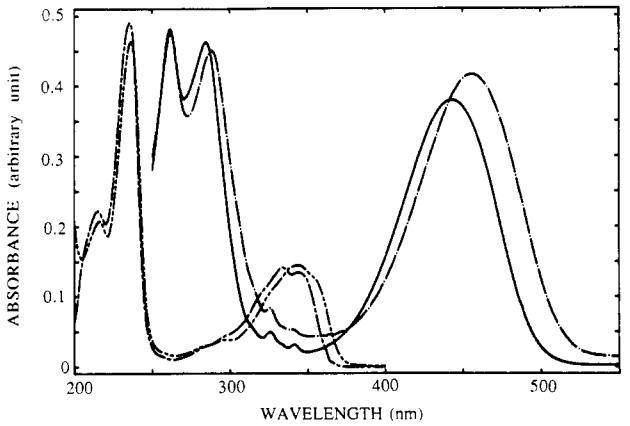


**Figure 2.** Absorption spectra of BNPI in EtOH (—) and $H_2O$/EtOH (4:1, v/v) (- · -) and of NPI in EtOH (- - -) and $H_2O$/EtOH (9:1, v/v) (- - - -). SNPI is not shown because it is essentially identical with BNPI.

valently bonded to macromolecular chain. The unusual shape of the GPC refractive index elution curves are similar to those reported by Dubin and Levy[20] and were ascribed to a Donnan equilibrium effect by these workers. We note that the addition of $NaNO_3$ was required to prevent the polymer from sticking to the GPC column.

**5. Purification of Quenchers.** The zwitterionic quencher 4,4′-bipyridinium 1,1′-bis(trimethylenesulfonate) (SPV, **3**; Chart I) was prepared by the method of Brugger et al.[21] and was purified by multiple precipitations in which methanol was added to an aqueous SPV solution. This was necessary to remove an acid species, which confused quenching studies by simultaneously quenching the excited state and lowering the pH of the solution, which increases the quantum yield of the fluorescence in the case of the polymer-bound chromophore (vide infra). $CH_3NO_2$ (MCB) was used as received, although this species also can slightly lower the solution pH.

## Results and Discussion

**1. Absorption and Emission Spectra of Model Compounds.** The absorption spectra of BNPI and NPI in ethanol and ethanol/water are given in Figure 2. The SNPI absorption is not shown because it is essentially identical with that of BNPI. For BNPI and SNPI there are two distinct bands in the ultraviolet and visible regions, respectively, whose positions are listed in Table II. The ultraviolet band has a distinct vibrational structure, but the visible band appears structureless. None of the model compounds are water soluble, but it is possible to carefully dilute ethanolic solutions with water up to a 9:1 volume ratio of water to ethanol before precipitation takes place. It was found that the visible absorption band of BNPI and SNPI is sensitive to the solvent composition, exhibiting a bathochromic shift with the addition of water and tending

**Table II**
**Absorption, Excitation, and Emission Spectral Peaks**

| substance | solvent | pH | absn peaks, nm {log $\epsilon^a$} | emission peak,[b] nm | $\phi_n$ |
|---|---|---|---|---|---|
| BNPI | EtOH | | 262, 284, 444 {4.20, 4.20, 4.13} | 529.3 529.3 | 0.59 0.59 |
| | $H_2O$/EtOH[a] | | 262, 286, 456 {4.23, 4.21, 4.17} | 544 | 0.34 |
| PBNAI-AA | $H_2O$ | 7.6 | 266, 290, 456 {4.23, 4.21, 4.17} | 547.0 | 0.085[d] |
| SNPI | EtOH | | 262, 284, 444 {4.46, 4.45, 4.37} | 530.4 | 0.64 |
| | $H_2O$/EtOH[c] | | 262, 288, 456 {4.46, 4.44, 4.39} | 546.0 | 0.35 |
| PSNAI-AA | $H_2O$ | 3.5 | 264, 290, 456 {4.37, 4.39, 4.39} | 549 | 0.067[d] |
| NPI | EtOH | | 236, 334, 344 {4.15, 4.10, 4.08} | 370, 385 | 0.037 |
| | $H_2O$/EtOH[e] | | 236, 346 {4.65, 4.15} | 387.5, 395.5 | 0.026 |
| PNAI-AA (low) | $H_2O$ | 4.6 | 236, 346 {4.65, 4.22} | 385, 397, 498.5 | 0.049 |
| PNAI-AA (high) | $H_2O$ | 6.3 | 236, 346 {4.65, 4.26} | 385.5, 397.5, 500 | 0.076 |

[a] Units of $\epsilon$ are $M^{-1}$ $cm^{-1}$. [b] Excited at the absorption peak of long wavelength band. [c] $H_2O$/EtOH (4:1, v/v) [d] Determined at pH = 5.0 and 4.7 for PBNAI-AA and PSNAI-AA, respectively. [e] $H_2O$/EtOH (9:1, v/v).

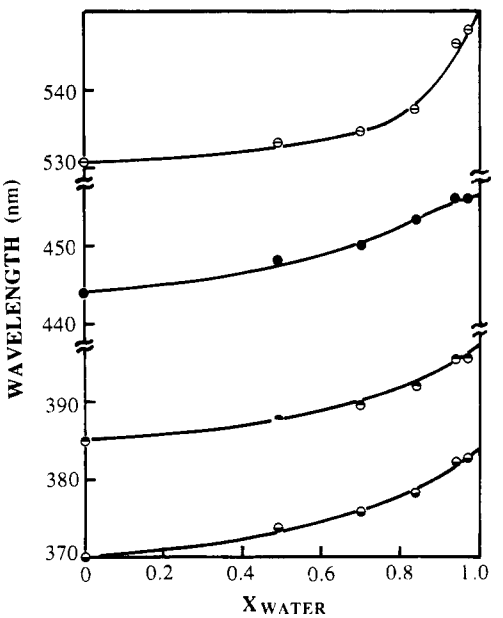


**Figure 3.** Solvent dependence of the emission and absorption peak position for SNPI and BNPI (● = absorption, ⊖ = emission). Solvent dependence of the two emission peaks of NPI (⊖, ⊖). $X_{water}$ is the mole fraction of water.

toward a constant wavelength of 456 nm for a water percentage greater than 80 vol % (these shifts are identical for BNPI and SNPI and are combined in Figure 3). We take this extrapolated value to be the peak position of the model compound in water. It is interesting that no spectral differences were found between BNPI and SNPI in ethanol or water, and these spectra are very similar to 4-amino-1,8-naphthalimides.[7,8] This demonstrates that the visible band of the 1,8-naphthalimide is essentially independent of the particular substituent group at the 4-position so long as some conjugation occurs with the aromatic system. This independence was also found in other photophysical properties (vide infra).

The absorption spectrum of NPI in ethanol is very different from the 4-substituted species (Figure 2), with the major long wavelength absorption peak at 344 nm instead of 444 nm. The fluorescence yield of NPI is also

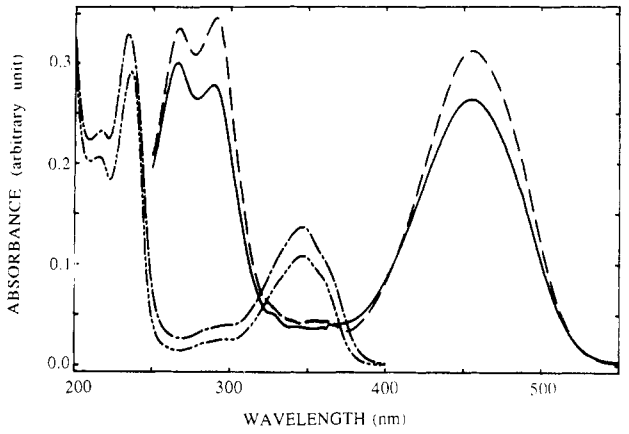


**Figure 4.** Absorption spectra for PBNAI-AA (—), PSNAI-AA (– –), and PNAI-AA (low, – · · –; high, – · –) in water at pH 7.5.

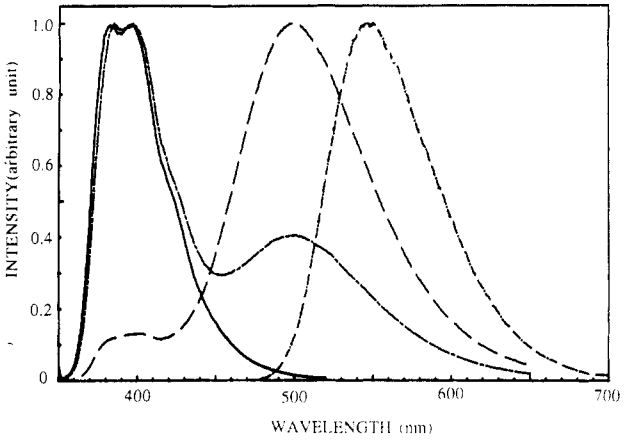


**Figure 5.** Emission spectra of PBNAI-AA (– · –) and PNAI-AA (low, – · –; high, – –) and NPI (—). PSNAI-AA and BNPI are not shown because they are essentially identical with PBNAI-AA.

lower than BNPI and SNPI (Table II) by a factor of ca. 20. Obviously the presence of a partially conjugated 4-substitution in these moieties produces a profound effect on their photophysics.

The extinction coefficient at the visible peak position of BNPI and SNPI also changes with solvent composition. The optical density extrapolated to pure water yields a molar extinction coefficient at the peak maximum of $1.51 \times 10^4$ and $2.62 \times 10^4$ $M^{-1}$ $cm^{-1}$ for BNPI and SNPI, respectively. For NPI the peak at 236 nm does not shift with solvent composition, nor is the extinction coefficient a function of solvent composition ($\epsilon_{236} = 4.43 \times 10^4$ $M^{-1}$ $cm^{-1}$).

The excitation spectrum is identical with the absorption spectrum, and the fluorescence spectrum is independent of the excitation for all model compounds. This means that all absorption peaks are intrinsic to the model compound. No concentration dependence of the emission spectrum was observed in any model compound solutions, nor was excimer fluorescence found (the fluorescence spectra are combined with the polymer spectra presented later in Figure 5). Upon addition of water, a bathochromic shift in the emission spectrum was observed (Figure 3). This behavior is very similar to the absorption shifts. At high water content, the emission wavelength tends to a constant value of 549 (±0.5) nm for both BNPI and SNPI. These extrapolated values are taken to be the emission peak wavelengths of BNPI and SNPI in water. While the fluoresence spectrum of NPI is very different from the substituted naphthalimides, the shift of the two peaks at 383.8 and 396.5 nm with solvent is similar to BNPI and SNPI (see Figure 3). The fluorescence quantum yields for all model compounds are given in Table II.

**2. Absorption and Emission Spectra of PBNAI-AA, PSNAI-AA, and PNAI-AA.** The absorption spectra of PBNAI-AA and PSNAI-AA in water are shown in Figure 4. There is a slight bathochromic shift for the UV band compared to the model compound in water/EtOH (4:1, v/v), while the visible bands are the same as that of the model compound (see Table II). The optical density at 456 nm was used to calculate the weight percentage of the naphthalimide on the polymer chain using the molar extinction coefficient of the model compound extrapolated to pure water (see the previous section). The composition was determined to be 3.9 and 2.8 mol % of the chromophore for PBNAI-AA and PSNAI-AA, which corresponds to 12.0 and 9.7 wt %, respectively. The excitation spectra of PBNAI-AA and PSNAI-AA in water are almost identical with the absorption spectra, and the emission spectra shape and peak position are independent of excitation wavelength, which indicates that the polymer sample is homogeneous. No excimer fluorescence was found for either polymer (see Figure 5).

Likewise the absorption (Figure 4) and excitation spectra for both PNAI-AA polymers were essentially identical with each other and very similar to the NPI model compound. When the extinction coefficient quoted above for NPI at 236 nm in water is used, the compositions of PNAI-AA (low) and PNAI-AA (high) were estimated to be 1.0 and 8.1 mol % of chromophore, respectively. The fluorescence spectra of these polymers are very different from those of PBNAI-AA and PSNAI-AA in that there is an obvious monomer ($\lambda_{max}$ at 385 and 397 nm) and excimer ($\lambda_{max} \approx$ 500 nm) component, whose ratio varies with composition (see Figure 5). Since this component is observed in the 1.0 mol % sample, which represents a lower loading than the PBNAI-AA or PSNAI-AA polymers, it seems likely that excimer formation is prevented in these latter polymers by the bulky 4-substituent.

**3. pH and Ionic Strength Dependence of Emission Intensity for PBNAI-AA and PSNAI-AA.** There is a weak pH dependence of the absorbance for dilute aqueous solution of PBNAI-AA and PSNAI-AA (<0.05 mg/mL). The much stronger pH dependence of the emission intensity, normalized to equal absorbance, is presented in Figure 6. The emission intensity for PBNAI-AA and PSNAI-AA is much more sensitive to the pH than the absorbance and displays an intensity jump across two pH units at pH 6–8 and 3–5, respectively. However, the emission intensity has no obvious pH dependence for the model compounds in water/ethanol and polymers with less than 1 chromophore/macromolecule. This suggests that the pH dependence of the emission intensity is the result of interactions between chromophores on the same chain.

The normalized absorbance for dilute aqueous solutions of PBNAI-AA and PSNAI-AA decreases only slightly with ionic strength, but the emission intensity decreases rapidly upon the initial addition of electrolyte. The extent of this effect depends on the pH of solution (Figure 7). This ionic strength dependence of the emission intensity was not observed in BNPI/water–EtOH (4:1, v/v) and SNPI/water–EtOH (4:1, v/v). In view of the spectral complexity of PNAI-AA, we did not explore its pH and ionic strength dependence.

**4. Fluorescence Decay of Model Compounds and Polymers.** The emission decay of BNPI and SNPI in EtOH and 4:1 v/v water/EtOH can be fit successfully by a single exponential. The lifetime data for these model

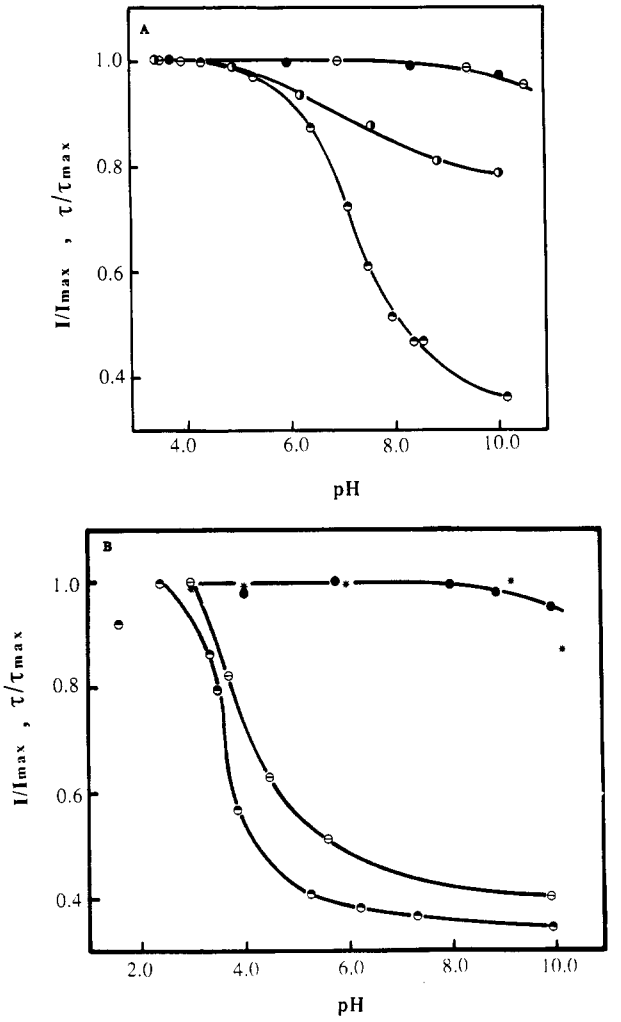


**Figure 6.** (A) pH dependence of normalized fluorescence intensity for BNPI (in 4:1 water/EtOH) (⊖), very low loading PBNAI-AA (●), and PBNAI-AA (3.9 mol %) (◓). Normalized $\langle\tau\rangle$ value for PBNAI-AA (3.9 mol %) (◑). (B) pH dependence of normalized fluorescence intensity for SNPI (in 4:1 water/EtOH) (*), very low loading PSNAI-AA (●), PSNAI-AA (2.8 mol %) (◓). Normalized $\langle\tau\rangle$ value for PSNAI-AA (2.8 mol %) (⊖).

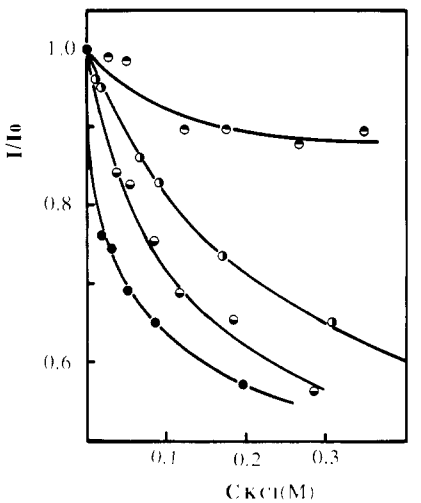


**Figure 7.** Ionic strength dependence of normalized emission intensity for BNAI-AA copolymer in $H_2O$ at pH 3.3 (◓), 7.6 (◑), and 10.0 (◓) and PSNAI-AA at pH 3.2 (●).

compounds are presented in Table III for different solvents. These data demonstrate that water shortens the emission lifetime of BNPI and SNPI, similar to the results reported by Pardo et al.[6] for 3-amino-1,8-naphthalimide in ethanol/water mixtures. However, the lifetime of the naphthalimides in 4:1 (v/v) water/EtOH is almost independent of the pH of the solution, unlike the results obtained by Pardo et al.[6]

**Table III**
**Emission Decay of Model Compounds[a]**

| substance | solvent | pH | lifetime, ns |
|---|---|---|---|
| BNPI | EtOH | | 9.1 |
| BNPI | water[b] | 3.8 | 5.4 |
| BNPI | water[b] | 7.0 | 5.4 |
| BNPI | water[b] | 9.7 | 5.4 |
| SNPI | EtOH | | 9.1 |
| SNPI | water[b] | 3.4 | 5.6 |
| SNPI | water[b] | 5.9 | 5.7 |
| SNPI | water[b] | 9.2 | 5.7 |
| SNPI | water[b] | 10.7 | 5.4 |
| NPI[d] | EtOH | | 0.5[c] |
| NPI[d] | water[b] | 7.0 | 2.1[c] |

[a] Excited at 445–455 nm with the $H_2$ lamp unless otherwise noted. [b] Water/EtOH (4:1, v/v). [c] Lifetimes agreed at 370 and 383 nm. [d] Excited at 293 nm with ps system.

**Table IV**
**pH Dependence of Emission Decay for PBNAI-AA, PSNAI-AA, and PNAI-AA (low)**

(a) PBNAI-AA[c]

| pH | $a_1/\tau_1$, ns | $a_2/\tau_2$, ns | $\tau$,[a] ns | $\langle\tau\rangle^b$ |
|---|---|---|---|---|
| 3.5 | 0.422/2.80 | 0.578/6.51 | 4.94 | 5.62 |
| 5.0 | 0.379/2.37 | 0.621/6.41 | 4.48 | 5.67 |
| 6.3 | 0.461/2.30 | 0.539/6.57 | 4.60 | 5.59 |
| 7.1 | 0.479/2.31 | 0.522/6.74 | 4.62 | 5.69 |
| 7.7 | 0.510/1.98 | 0.490/6.78 | 4.33 | 5.66 |
| 8.0 | 0.594/1.93 | 0.406/6.96 | 3.97 | 5.51 |
| 10.1 | 0.606/1.95 | 0.394/6.80 | 3.86 | 5.31 |

(b) PSNAI-AA[c]

| pH | $a_1/\tau_1$, ns | $a_2/\tau_2$, ns | $\tau$,[a] ns | $\langle\tau\rangle^b$ |
|---|---|---|---|---|
| 3.0 | 0.560/2.49 | 0.440/5.97 | 4.02 | 4.76 |
| 3.7 | 0.676/2.00 | 0.324/6.08 | 3.32 | 4.42 |
| 4.5 | 0.746/1.40 | 0.254/5.91 | 2.55 | 4.05 |
| 5.6 | 0.832/1.30 | 0.168/5.76 | 2.05 | 3.88 |
| 9.9 | 0.845/1.16 | 0.155/4.25 | 1.64 | 2.40 |

(c) PNAI-AA (low)[d]

| pH | $a_1/\tau_1$ | $a_2/\tau_2$ | $a_3/\tau_3$ | $\tau^a$ | $\langle\tau\rangle^b$ |
|---|---|---|---|---|---|
| | | monomer (383 nm) | | | |
| 3.2 | 0.728/0.238 | 0.265/0.620 | 0.007/1.82 | 0.351 | 0.477 |
| 4.25 | 0.717/0.253 | 0.278/0.674 | 0.005/2.48 | 0.382 | 0.537 |
| 6.0 | 0.555/0.199 | 0.436/0.726 | 0.009/2.073 | 0.445 | 0.650 |
| 7.75 | 0.656/0.116 | 0.266/0.635 | 0.079/1.263 | 0.344 | 0.702 |
| 9.1 | 0.747/0.088 | 0.221/0.659 | 0.033/1.677 | 0.266 | 0.727 |
| | | excimer (500 nm) | | | |
| 3.2 | 0.544/0.377 | 0.188/5.27 | 0.268/16.0 | 5.49 | 13.5 |
| 4.25 | 0.544/0.441 | 0.198/6.09 | 0.259/16.5 | 5.70 | 13.6 |
| 6.0 | 0.387/0.546 | 0.387/4.96 | 0.342/16.0 | 7.16 | 13.3 |
| 7.75 | 0.321/1.10 | 0.400/5.23 | 0.279/15.4 | 6.73 | 11.5 |
| 9.1 | 0.386/1.28 | 0.400/5.18 | 0.214/14.6 | 5.68 | 9.96 |

[a] $\tau = \sum a_i\tau_i$ where $\sum a_i = 1$. [b] $\langle\tau\rangle = \sum a_i\tau_i^2/\sum a_i\tau_i$. [c] Determined with a flash-lamp system using 456-nm excitation. [d] Determined with a picosecond system using 293-nm excitation.

The emission decay of PBNAI-AA and PSNAI-AA in water is different from that of their model compounds and can only be fit by a double experimental. The decay parameters and average lifetimes of PBNAI-AA and PSNAI-AA at different pHs are listed in Table IV. It is seen that the average lifetime of substituted naphthalimides in water decreases with pH, especially for PSNAI-AA. Since the model compounds do not display this behavior, we conclude that both the double-exponential decay and the pH dependence of the average lifetime arise from covalently binding these chromophores to the cat-

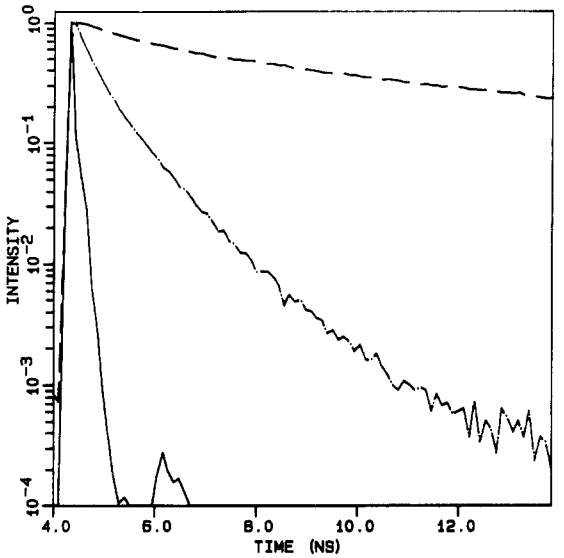


**Figure 8.** Fluorescence decay of PNAI-AA (low) of monomer (- · -, 383 nm) and excimer (- -, 500 nm). The instrument response function is also indicated (—).

**Table V**
**Radiative Rate Constant[a]**

| substance | solvent (pH) | $k_{rad}$, $\times 10^{-7}$ $s^{-1}$ |
|---|---|---|
| BNPI | EtOH | 6.5 |
| | $H_2O$/EtOH[b] | 6.4 |
| PBNAI-AA | $H_2O$ (7) | 1.8 |
| SNPI | EtOH | 7.0 |
| | $H_2O$/EtOH[b] | 6.1 |
| PSNAI-AA | $H_2O$ (3.5) | 2.0 |
| NPI | EtOH | 7.5 |
| | $H_2O$/EtOH[b] | 1.3 |
| PNAI-AA | $H_2O$ (7) | ca. 2[b] |

[a] Using eq 1 and the data from Tables II–IV. [b] Estimated roughly from the average of the monomer and excimer lifetimes.

ionic polymers. The fluorescence decay of PNAI-AA is complicated by the presence of the excimer emission. For this polymer it was necessary to use a three-exponential fitting function (Table IV). We note that no rise time was observed for the excimer decay (Figure 8), indicating either that the excimer results from pairs of chromophores appropriately positioned to form an excimer or that there is very rapid energy transfer to these excimer-forming sites. At pH 7 the average monomer lifetime (observed at 383 nm) is ca. 0.3 ns, while for the excimer (observed at 500 nm) the average lifetime was ca. 5–7 ns.

The radiative rate constant can be obtained by combining the quantum yield data in Table II with the average lifetime data in Tables III and IV:

$$k_{rad} = \phi_{fl}/\tau \quad (1)$$

Using this formula, we find that $k_{rad}$ is essentially identical and independent of solvent for the 4-substituted model compounds (Table V), but $k_{rad}$ is significantly diminished for the polymer-bound chromophores. We will argue later that this implies a static quenching mechanism for the polymer case. For NPI $k_{rad}$ is dramatically solvent dependent. No clear determination can be made for PNAI-AA because of the independent monomer and excimer components of the emission.

**5. Fluorescence Quenching Studies.** In previous studies of aromatic chromophores bound to water-soluble polymers, we and others have found it useful to characterize the effect of the polymer on excited-state quenching.[13,14,22] In general, one expects that as the polymer coil contracts the chromophores will tend to be protected from quencher species unless the quencher is solubilized by the collapsed coil. Additionally, the state of charge of the polymer may strongly effect the concentration in the region of the coil of a charged or highly polar species. We have also been interested in the use of polymer-bound chromophores as aqueous photoredox reagents in which an excited state can transfer an electron to or from a quenching species, followed by charge pair separation, which results in the storage of a fraction of the absorbed photon energy. Thus, we examined the quenching of these chromophores with a zwitterionic viologen, 4,4′-bipyridinium 1,1′-bis(trimethylene sulfonate) (SPV, **3**), and $CH_3NO_2$, both of which have been used in similar studies in the past.[14,15]

**Table VI**
**SPV Fluorescence Quenching Data**

| substance | pH | $K_{SV}$, $M^{-1}$ | $\langle\tau\rangle$,[a] ns | $k_q$, $\times 10^{-9}$ $M^{-1}$ $s^{-1}$ |
|---|---|---|---|---|
| BNP[b] | | 28.1 | 5.4 | 5.2 |
| SNPI[b] | | 28.0 | 5.7 | 4.9 |
| PBNAI-AA | 3.4 | 27.3 | 5.6 | 4.9 |
| | 4.2 | 27.6 | 5.6[c] | 4.9 |
| | 5.3 | 24.2 | 5.7 | 4.3 |
| | 6.4 | 17.3 | 5.6 | 3.1 |
| | 7.7 | 12.1 | 5.7 | 2.1 |
| | 8.5 | 6.44 | 5.5 | 1.2 |
| | 9.3 | 7.01 | 5.5 | 1.3 |
| PSNAI-AA | 3.5 | 38.0 | 4.4 | 8.6 |
| | 4.8 | 34.8 | 4.1 | 8.6 |
| | 5.4 | 31.1 | 3.4 | 9.2 |
| | 6.5 | 17.18 | 2.4[c] | 7.4 |
| | 7.5 | 14.8 | 2.4[c] | 6.2 |
| NPI[b] | | 9.1 | 2.1 | 4.3 |
| PNPI-AA[d] | 3.5 | 7.9 | 0.48 | 16 |
| | 5.6 | 7.9 | 0.65 | 12 |
| | 7.6 | ca. 0 | 0.7 | ca. 0 |
| PNPI-AA[e] | 3.5 | 11.0 | 13.5 | 0.82 |
| | 5.6 | 5.5 | 13.3 | 0.41 |
| | 7.6 | 6.4 | 11.5 | 0.56 |

[a] See eq 3. $\langle\tau\rangle$ computed by using data in Tables III and IV. [b] In $H_2O$/EtOH (4:1, v/v). [c] Estimated by interpolation of lifetime data at different pHs (from Table IV). [d] Monomer component, for low-loading polymer. [e] Estimated from corrected excimer-quenching curve: $(I_0^E/I^E)(I^M/I_0^M) = 1 + K_{SV}[Q]$ (see ref 25), for low-loading polymer.

In all cases the quenching could be treated by standard Stern–Volmer kinetics, in which the intensity of the steady-state fluorescence obeys the following expression:

$$I_0/I = 1 + K_{SV}[Q] \quad (2a)$$

$$= 1 + k_q\tau[Q] \quad (2b)$$

The fact that a simple linear quenching behavior is obeyed suggests that the quenching species is not preferentially adsorbed by the polymer coil. For simple homogeneous systems, $k_q$ is a second-order rate constant and $\tau$ is the excited-state lifetime. We have argued previously[23] that if there is an ensemble of environments for a chromophore that differ in excited-state lifetime but not $k_q$ or the radiative rate constant, then $\tau$ in eq 2b should be replaced with

$$\langle\tau\rangle = \sum a_i\tau_i^2/\sum a_i\tau_i \quad (3)$$

The quenching data for SPV are presented in Table VI. As can be seen, the model compounds are quenched at approximately what one would estimate for the diffusion-controlled rate. At low pH the polymers are quenched with equal or greater efficiency. As the pH increases, the $K_{SV}$ value for both polymers decreases (Figure 9), as one might expect if the chromophore is protected from a quenching species. However, the dependence of the lifetime is quite different for PBNAI-AA and PSNAI-AA, with the latter

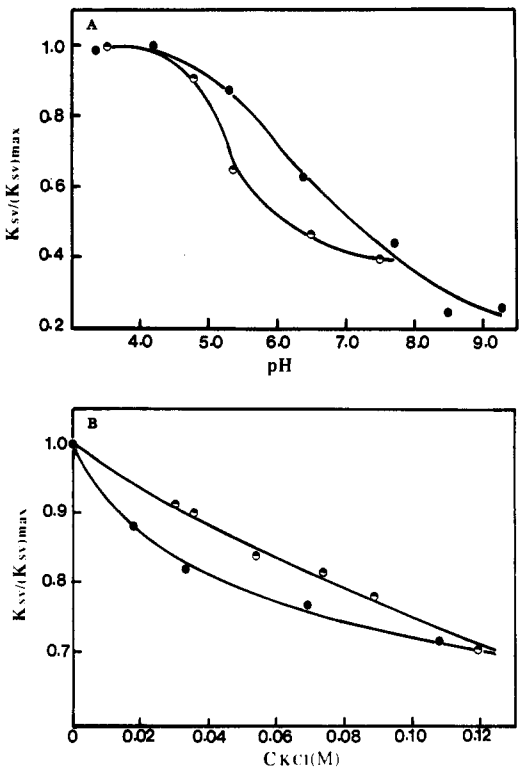


**Figure 9.** Plot of normalized $K_{SV}$ as a function of (A) pH and (B) ionic strength at pH 4.1 for PBNAI-AA (●) and PSNAI-AA (⊖).

exhibiting a strongly pH-dependent $\langle\tau\rangle$ value (Table IV). The net result is that $k_q$ is found to decrease strongly with increased pH for PBNAI-AA while little or no change occurs for PSNAI-AA. We speculate that in the former case the neutral chromophore is protected from the SPV by the coil as contraction occurs while this is much less effective for the anionic PSNAI-AA chromophores. An analogous effect is observed for PBNAI-AA and PSNAI-AA at low pH as a function of ionic strength. As is seen in Figure 9, $K_{SV}$ decreases systematically with KCl concentration. This is likely to be the effect of both coil contraction and the screening of the polycation electrostatic field from the SPV.

For PNAI-AA the quenching study is complicated by the presence of the excimer. If we assume that the monomer excited state is the sole precursor of the excimer (i.e., no direct excitation of the excimer-forming site), then the excimer quenching expression should be[24]

$$(I_0^E/I^E)(I^M/I_0^M) = 1 + K_{SV}^E[Q] \quad (4a)$$

$$= 1\, k_q^E\langle\tau_E\rangle[Q] \quad (4b)$$

When the PNAI-AA data are treated in this fashion, a good linear fit is obtained and it is these values that are presented in Table VI. We note that $k_q^M$ at low pH is somewhat larger than that for the visible band of PBNAI-AA and PSNAI-AA, while $k_q^E$ is much smaller. Since the nature of the excited states is rather different for PNAI-AA than the other polymers, this may be either an electronic effect (e.g., photoredox energies) or a steric effect (e.g., excimers are better shielded from the solvent). The precipitous drop for the PNAI-AA monomer between pH 5.6 and 7.6 may reflect the inaccessibility of monomer excited states, which are not appropriately positioned to form excimers with a neighboring chromophore. We note that at this pH there is very little residual monomer fluorescence.

**Table VII**
**$CH_3NO_2$ Fluorescence Quenching Data**

| substance | pH | $K_{SV}$, $M^{-1}$ | $\langle\tau\rangle$,[a] ns | $k_q$, $\times10^{-8}$ $M^{-1}$ $s^{-1}$ |
|---|---|---|---|---|
| BNPI[b] | | 5.2 | 5.4 | 9.7 |
| PBNAI-AA | 3.9 | 1.6 | 5.6 | 2.8 |
| PBNAI-AA | 7.0 | 0.58 | 5.6 | 1.0 |
| SNPI[b] | | 5.5 | 5.7 | 9.6 |
| PSNAI-AA | 3.7 | 1.4 | 4.4 | 3.2 |
| PSNAI-AA | 7.5 | 0.17 | 2.4 | 0.71 |

[a] See eq 3. $\langle\tau\rangle$ computed by using data of Tables III and IV. [b] In $H_2O$/EtOH (4:1, v/v).

For quenching of PBNAI-AA and PSNAI-AA by $CH_3NO_2$ a similar effect of pH is observed;[25] i.e., at a higher pH, the $k_q$ value is decreased (see Table VII). We also note that $k_q$ for the polymer at low pH is lower by a factor of 3 compared to the model compound. This is expected because of the low diffusion constant of the polymer-bound chromophore and the possible steric hindrance of the polymer chain. In fact, it is surprising that the SPV $k_q$ values for the model compound and polymer at low pH in Table VI are so similar. We speculate that this arises from some clustering of the zwitterionic SPV in the vicinity of the polycation.

## Discussion

Our primary motivation in the present work was to explore a new class of polymer-bound chromophores that absorb in the visible and that were expected to have a high fluorescent yield. By analogy to known model compounds, the presence of a conjugated substituent at the 4-position of a 1,8-naphthalimide has a profound effect on the spectroscopic properties of the chromophore.

For the 4-substituted PBNAI-AA and PSNAI-AA the fluorescence quantum yield is much lower than the model compounds (Table II), yet there is only a modest decrease in the average fluorescence lifetime. Despite the fact that the extinction coefficients of the model and polymer-bound chromophores are essentially identical (Table II) and the near independence of the radiative rate constant to solvent for the model compounds, the apparent radiative rate constant is greatly decreased for the polymer case (Table V). Additionally the fluorescence decay for the polymer-bound chromophores is highly nonexponential (Table IV), which is consistent with a heterogeneous environment, among other possibilities. It seems likely to us that the decreased fluorescence quantum yield is the result of chromophore–chromophore interactions that lead to self-quenching without excimer fluorescence. In partial support of this idea, the polymer with an equivalent loading of the unsubstituted 1,8-naphthalimide does exhibit an excimer band, and the overall fluorescence quantum yield is slightly higher for PNAI-AA than NPI (Table II). Other than possible steric effects, it is not obvious to us why the result of chromophore–chromophore interactions would be so different for these two cases. One would expect the SNPI moiety to be different from BNPI in this regard, but we do not find this to be the case. Since these phenomena are not a function of overall concentration, we assume that these chromophore interactions are intrapolymer, but this has not been explored in detail to date.

The pH and ionic strength not only affect the photophysical properties of the polymer-bound naphthalimides but also modify the second-order quenching constant ($k_q$) for two uncharged quenchers, SPV (3) and $CH_3NO_2$. In all cases $k_q$ decreases either as the pH is increased or, for lower pHs, as the ionic strength is increased. This can be the result of two complementary effects: (1) diminution of the electrostatic field around the poly(allylamine), which

in turn decreases any tendency of the polar quenchers to cluster around the polymer, and (2) collapse of the polymer coil, which can serve to protect the chromophores. Since the chromophores are not hydrophilic, we assume that they tend to be minimally exposed to the aqueous phase.

In earlier fluorescence quenching studies of polyanions containing a small mole percent of aromatic chromophore, it has been found that there is a significant component of static quenching, which is manifested in part by a nonlinear Stern–Volmer plot (see eq 2). This was not observed in the present case. While this does not constitute proof that the quenching mechanism is diffusive, it does suggest that the kinetics of quenching for the zitterionic SPV might depend on the portion of this molecule that is strongly attracted to the polyelectrolyte (cf. $-SO_3$ or pyridinium).

There remains a great deal more that can be explored for this class of polymer-bound chromophores in the future: (1) Can a sufficiently high loading of chromophore be achieved to effect efficient down-chain electronic energy transfer, or will self-quenching dominate the photophysics? This will be strongly influenced by the supporting polymer chain. (2) Can these chromophores participate in photoredox chemistry? In particular, they are relatively easily reduced (see Table I), so the excited state should be an effective photooxidizer. All these chromophores have some potential to act as a fluorescent probe for solvent polarity, although the changes that occur are not exceptional compared to other well-known molecules such as 8-anilinonaphthalene-1-sulfonate.[26]

**Acknowledgment.** This work has been supported by the Robert A. Welch Foundation (Grant F-356) and the National Science Foundation Polymers Program (Grant DMR-86-8614252). We thank Dai-Ting Rong for making the electrochemical measurements and Doug Kiserow for carrying out the picosecond fluorescence lifetime measurements.

## References and Notes

(1) (a) Bai, F.; Chang, C. H.; Webber, S. E. *Macromolecules* **1986**, *19*, 2484. (b) Itoh, Y.; Webber, S. E.; Rodgers, M. A. J. *Macromolecules* **1989**, *22*, 2766. (c) Webber, S. E. Photon Harvesting Polymers *Chem. Rev.*, in press.
(2) Steward, W. W. *Nature* **1981**, *292*, 17.
(3) Marling, J. B.; Hawley, J. G.; Liston, E. M.; Grant, B. *Appl. Opt.* **1974**, *13*, 2317.
(4) Middleton, R. W.; Parrick, J. *J. Heterocycl. Chem.* **1985**, *22*, 1567.
(5) Middleton, R. W.; Parrick, J. *J. Heterocycl. Chem.* **1986**, *23*, 849.
(6) Pardo, A.; Poyato, J. M. L.; Camacho, J. J.; Espelosin, R. H.; Fernandez-Alonso, J. I. *J. Mol. Struct.* **1986**, *142*, 147.
(7) Pardo, A.; Martin, E.; Poyato, J. M. L.; Camacho, J. J. *J. Photochem. Photobiol., A* **1987**, *41*, 69.
(8) Pardo, A.; Poyato, J. M. L.; Martin, E. *J. Photochem.* **1987**, *36*, 323.
(9) Pardo, A.; Companario, J.; Polyato, J. M. L.; Camacho, J. J.; Reyman, D.; Martin, E. *THEOCHEM* **1988**, *166*, 463.
(10) Pardo, A.; Poyato, J. M. L.; Martin, E.; Camacho, J. J.; Reyman, D.; Brana, M. F.; Castellano, J. M. *J. Photochem. Photobiol. A* **1989**, *46*, 323.
(11) Pardo, A.; Martin, E.; Poyato, J. M. L.; Camacho, J. J.; Guerra, J. M.; Weigand, R.; Brana, M. F.; Castellano, J. M. *J. Photochem. Photobiol. A* **1989**, *48*, 259.
(12) See, for example: *Structure and Properties of Ionomers*; Pineri, M., Eisenberg, A., Eds.; NATO Advanced Study Institute Series 198; Reidel: Dordrecht, 1987.
(13) (a) Chu, D.-Y.; Thomas, J. K. *Macromolecules* **1984**, *17*, 2142. (b) Bednar, B.; Morawetz, H.; Shafer, J. A. *Macromolecules* **1985**, *18*, 1940. (c) Horsky, J.; Morawetz, H. *Makromol. Chem.* **1988**, *189*, 2475.
(14) Delaire, J. A.; Rodgers, M. A. J.; Webber, S. E. *J. Phys. Chem.* **1984**, *88*, 6219.
(15) Stramel, R. D.; Webber, S. E.; Rodgers, M. A. J. *J. Phys. Chem.* **1988**, *92*, 6625.
(16) See for example: Ford, W. E.; Kamat, P. V. *J. Phys. Chem.* **1987**, *91*, 6373 and references therein.
(17) Demas, J. N.; Crosby, G. A. *J. Phys. Chem.* **1971**, *75*, 991.
(18) Melhuish, W. H. *J. Phys. Chem.* **1961**, *65*, 229.
(19) O'Conner, D. V.; Phillips, D. *Time Correlated Single Photon Counting*; Academic Press: New York, 1984.
(20) Dubin, P. L.; Levy, I. J. *J. Chromatogr.* **1982**, *235*, 377.
(21) Brugger, P. A.; Grätzel, M.; Guarr, T.; McLendon, G. *J. Phys. Chem.* **1982**, *86*, 944.
(22) Webber, S. E. *Macromolecules* **1986**, *19*, 1658.
(23) Bai, F.; Chang, C.-H.; Webber, S. E. *Macromolecules* **1986**, *19*, 588.
(24) Webber, S. E.; Avots-Avontins, P. E.; Deumié, M. *Macromolecules* **1981**, *14*, 105.
(25) We note that addition of significant amounts of $CH_3NO_2$ can significantly lower the pH, which in turn affects the fluorescence quantum yield at higher pHs. Consequently, only pHs below 7 were examined.
(26) (a) Turner, D. C.; Brand, L. *Biochemistry* **1968**, *7*, 3381. (b) Wong, M.; Thomas, J. K.; Grätzel, M. *J. Am. Chem. Soc.* **1976**, *98*, 229. (c) Treloar, F. E. *Chem. Scr.* **1976**, *10*, 219.

**Registry No.** 1 (R = Br), 100865-05-2; 1 (R = $SO_3^-$·$K^+$), 130326-26-0; 1 (R = H), 6914-61-0; 3, 77951-49-6; BNA, 81-86-7; SNA, 71501-16-1; propylamine, 107-10-8; 1,8-naphthalic anhydride, 81-84-5.